The Catalytic Cracking of Hydrocarbons in a Riser Simulator: The Effect of Catalyst Accessibility and Acidity

K.A. Mahgoub and S. Al-Khattaf*

Department of Chemical Engineering, King Fahd University of Petroleum & Minerals, Dhahran 31261, Saudi Arabia.

Different catalysts based on Y-zeolite, ZSM-5 and amorphous kaolin were prepared and characterized. The catalytic cracking of 1,3,5-triisopropylbenzene (1,3,5-TIPB), 1,4-diisopropylbenzene (1,4-DIPB) and n-dodecane were used to investigate the effect of catalyst nature on the catalytic performance. Cracking the largest molecule (1,3,5-TIPB) using the kaolin, with largest pore structure, was found to be most efficient although it has lowest acidity. On the contrary, cracking of n-dodecane was found to be very efficient using catalyst based on ZSM-5 zeolite. Koalin catalyst produces more cumene when used for cracking 1,4-DIPB and 1,3,5-TIPB than the zeolite catalyst. Benzene selectivity was highest for ZSM-5 catalyst and high reaction temperature. Generally, cracking of 1,3,5-TIPB produces more coke followed by 1,4 DIPB and least is n-dodecane. Amorphous kaolin was found to produce less coke than both USY and ZSM-5 zeolites; however kaolin was found completely inactive in cracking n-dodecane.

---

*Corresponding author. Tel.: +966-3-860 1429; Fax: +966-3- 860 4234
E-mail address: skhattaf@kfupm.edu.sa

1. Introduction

The FCC process is one of the most important processes for gasoline production. FCC processes can use different feeds to increase the product value. The basic mechanism involves the formation of carbenium ions that can lead to different reactions. These reactions include isomerization, B-scission, dealkylation, transalkylation and hydrogen transfer reaction. While, olefin cracking rate is highest among hydrocarbon, paraffin catalytic cracking rate is the lowest.[1]

The FCC catalysts are based on Y-zeolites as main component and on ZSM-5 as additive. These zeolites are bounded individually in a spray-dried matrix such as silica-alumina. In catalytic cracking hydrocarbon molecules have to diffuse through this matrix, then to the zeolite pore structure. While diffusion in the catalyst matrix belongs to the well-known Knudsen regime, diffusion in zeolites falls into the configurational regime.[2-5] This kind of diffusion is a process with activation energy substantially larger than the other diffusion types.[2] However, it essential not to view hydrocarbon molecules as rigid bodies.[6] Even if molecule critical diameters are greater than the zeolite super cage, these hydrocarbon molecules can still manage to diffuse inside the zeolite structure. However, there is a cut off size for each zeolite. Molecules with bigger size than this cut off size can not transport inside this particular zeolite.[2,6] For example, molecules with a critical diameter up to 10.2 Å can enter Y-zeolite.[2] Thus it is expected that 1,3,5-TIPB (critical diameter 9.5 Å) can barely manage to enter Y-zeolite[3,4] but not ZSM-5 and 1,4-DIPB (with 6.8 Å critical diameter) can mange to diffuse through the Y-zeolite, and can also diffuse, but with difficulty, through ZSM-5.

Regarding the catalytic cracking of isopropyl-benzene, it is established that the cleavage of the propyl group from the benzene ring is the main reaction pathway with the benzene ring remaining unaltered.[7] Moreover, transalkylation, disproportionation, isomerization, and coke formation are other reactions which reported to take place beside the cracking reaction.[3,4,7] Recently Al-Khattaf and de Lasa[3,4] cracked cumene and 1,3-DIPB and 1,3,5-TIPB using small and large Y-zeolite crystal size. They reported that cumene has no diffusion limitation inside Y-zeolite while 1,3,5-TIPB showed a clear diffusion obstacle at low temperature. Modeling the catalytic cracking of 1,3,5-TIPB was

carried out in other study using the riser simulator.[4] Furthermore **n**-hexadecane and 1,3,5-TIPB were used to confirm the diffusivity effect on zeolite performance.[8] It was found that accessibility to internal acid sites influences both catalyst activity and selectivity. Furthermore, the extra large pore zeolite MCM-41 yielded higher conversion of 1,3,5-TIPB than Y-zeolite.

ZSM-5 is a typical FCC additive due to its acidity and shape selectivity. The performance of ZSM-5 as FCC additive and the factors that can influence its activity and selectivity have been addressed by a great number of researchers.[9-17] It is reported that adding ZSM-5 additives promotes higher ratio of cracking to hydrogen transfer reactions than Y-zeiolite.[18] Furthermore, adding ZSM-5 to catalytic crackers had little effect on the heavier components such as aromatic compounds.[19] This can be viewed based on the small ZSM-5 pores which are in a range of 5-6 Å allowing normal paraffin and olefin to penetrate and then reacted.

In most of the case the microactivity test (MAT) was used to evaluate the ZSM-5 performance.[9,14-16] For example, it is well established that the addition of ZSM-5 to FCC riser will increase the octane number and decreases gasoline yield. Also an increase in C3-C4 gases was reported upon adding ZSM-5.[19] This reduction in gasoline will be mainly on the expense of the parrafinc and olefinic compounds in the gasoline range. In general, the main role of ZSM-5 as an additive is to crack and isomerize C5 + olefins.[19] The efficiency of ZSM-5 in converting normal hydrocarbons decreases with increasing carbon atom due to the difficulty of long chain in diffusion inside the tiny zeolite pores.[1] Biswass and Maxwell[20] used USY alone and a combination of USY/ZSM-5. It was reported the catalyst combination produced higher branched structure with higher RON and MON. Furthermore Ataini et al[21] added 10 wt% ZSM-5 in VGO catalytic cracking. Their results showed a significant increase in C3-C4 gases associated with a decrease in gasoline yield. The mass of gases increased was found to be equivalent to the decreased gasoline mass.[21] Using high reaction temperature and high ZSM-5 additive (up to 20 wt %) can further increase the C3-C4 yield. Moreover, ZSM-5 has the advantage of low deactivation tendency compared to the other zeolites.[22]

Recently, Corma et al[23] have used two catalysts one is based on the commercial FCC catalyst, which is based on Y-zeolite, and the other is based on the commercial FCC

additive, which is based on the ZSM-5. For the same reaction conditions, ZSM-5 gave higher conversion when light straight naphtha was used as feed. This higher conversion was obtained although ZSM-5 catalyst has lower acidity than Y-zeolite based catalyst. The higher ZSM-5 conversion was attributed to the smaller pore diameter of ZSM-5 compared to Y-zeolite which produces a larger confinement effect of the reactant which leads to enhance the turnover rate.[23]

Using ZSM-5 in FCC plants as an additive has gained huge significance to increase both octane number and C3-C4 olefins. Thus it is essential to understand the cracking behavior of this zeolite with different model compounds at different reaction conditions. Furthermore, a comparison with FCC catalyst based on Y-zeolite and amorphous catalyst is an objective of this study. The cracking of alkylarmatics represented by 1,3,5-triisopropylbenzene (1,3,5-TIPB), LCO range, and 1,4-diisopropylbenzene (1,4-DIPB), gasoline range, and that of the normal paraffin, C12 (n-dodecane) are going to be carried out using the Riser Simulator. The cracking of these molecules, using the suggested three catalysts, is of great importance because of its potential industrial applicability.

2. **Experimental Section**

2.1 The Riser Simulator. All the experimental runs were carried out in the riser simulator. This reactor is novel bench scale equipment with internal recycle unit invented by de Lasa[24] to overcome the technical problems of the standard micro-activity test (MAT). For example, the low olefinity obtained from MAT reactor, due to its higher reaction time (> 75 s) as compared to the riser (< 15 s), non uniform coke deposition (150 mm long catalyst bed), and temperature/concentration gradient, which are eliminated by the well-mixed characteristics and intense fluidization of the riser simulator. The riser simulator is fast becoming a valuable experimental tool for reaction evaluation involving model compounds[25-27] and also for testing and developing new fluidized catalytic cracking in vacuum gas oil cracking.[26, 27] The riser simulator consists of two outer shells, the lower section and the upper section, which allow one to load or to unload the catalyst easily, as illustrated in Fig. 1. The reactor was designed in such a way that an annular space is created between the outer portion of the basket and the inner part of the reactor

shell. A metallic gasket seals the two chambers with an impeller located in the upper section. A packing gland assembly and a cooling jacket surrounding the shaft provide support for the impeller. Upon rotation of the shaft, gas is forced outward from the center of the impeller towards the walls. This creates a lower pressure in the center region of the impeller, thus inducing flow of gas upward through the catalyst chamber from the bottom of the reactor annular region where the pressure is slightly higher. The impeller provides a fluidized bed of catalyst particles as well as intense gas mixing inside the reactor. A detailed description of various riser simulator components, sequence of injection and sampling can be found in work by Kraemer.[27]

2.2. Materials. Commercial Y- zeolite having a Si/Al atomic ratio of 2.6 provided by Tosoh Co. Japan was used in this work. The as-synthesized Na zeolite was ion exchanged with NH_4NO_3 to replace the Na cation with NH_4^+. Following this, NH_3 was removed and the H form of the zeolite was spray-dried using kaolin as the filler and a silica sol as the binder, Catalysts and Chemicals Industries Co. Japan supplied both materials. The resulting 60 μm catalyst particles had the following composition: 30 wt % zeolite, 50 wt % kaolin, and 20 wt % silica. The process of Na removal was repeated for the pelletized catalyst. Following this, the catalyst was calcined at 600^{o}C for 2 h. Finally, the fluidizable catalyst particles (60 μm average size) were treated with 100% steam at 780 ^{o}C for 6 hr to obtain the dealuminated Y- zeolites (designated SB). GKF-3 was prepared in the same manner but ZSM-5 zeolite (30 wt %) was added instead of Y-zeolite. It has to be mentioned that this catalyst (GKF-3) was not steamed. The third catalyst used in the present study is based on kaolin.

2.3. Catalyst characterization. The BET surface area was measured according to the standard procedure ASTM D-3663 using Sorptomatic 1800 Carlo Erba Strumentazione unit, Italy. The acid property of the catalyst was characterized by NH_3 temperature-programmed desorption (NH_3-TPD). In all the experiments, 50 mg of sample was outgassed at 400 ^{o}C for 30 min in flowing He and then cooled down to 150 ^{o}C. At that temperature, NH_3 was adsorbed on the sample by injecting pulses of 2 μl/pulse. The injection was repeated until the amount of NH_3 detected was the same for the last two

injections. After the adsorption of NH_3 was saturated, the sample was flushed at 150 ^oC for 1 h with He to remove excess NH_3, and then the temperature was programmed at 30 ^oC/min up to 1000 ^oC in flowing helium at 30 ml/min. Flame ionization detector was used to monitor the desorbed NH_3. The ratio of Lewis acid to Bronsted acid was measured by pyridine adsorbed FTIR spectroscopy.

2.4. Procedure. Regarding the experimental procedure in the riser simulator, an 80 mg portion of the catalyst was weighed and loaded into the riser simulator basket. The system was then sealed and tested for any pressure leaks by monitoring the pressure changes in the system. Furthermore, the reactor was heated to the desired reaction temperature. The vacuum box was also heated to around 250 ^oC and evacuated at around 0.5 psi to prevent any condensation of hydrocarbons inside the box. The heating of the riser simulator was conducted under continuous flow of inert gas (Ar), and it usually takes a few hours until thermal equilibrium is finally attained. Meanwhile, before the initial experimental run, the catalyst was activated for 15 min at 620 ^oC in a stream of Ar. The temperature controller was set to the desired reaction temperature, and in the same manner, the timer was adjusted to the desired reaction time. At this point the GC is started and set to the desired conditions.

Once the reactor and the gas chromatograph have reached the desired operating conditions, the feedstock was injected directly into the reactor via a loaded syringe. After the reaction, the four-port valve immediately opens, ensuring that the reaction was terminated and the entire product stream sent online to the analytical equipment via a preheated vacuum box chamber.

2.5. Analysis. The riser simulator operates in conjunction with a series of sampling valves that allow, following a predetermined sequence, one to inject reactants and withdraw products in short periods of time. The products were analyzed in an Agilent 6890N gas chromatograph with a flame ionization detector and a capillary column INNOWAX, 60-m cross-linked methyl silicone with an internal diameter of 0.32 mm.

3. **Results and Discussion**

3.1. Catalyst Characterization. The physico-chemical properties of the catalyst used in this study are presented in Table 1. Figure 2 shows the x-ray diffraction for the three used catalysts. This figure reveals the type of material (amorphous, Y-zeolite, and ZSM-5 zeolite) embedded in an amorphous matrix. The total acidity for each catalyst was determined by NH_3 adsorption (TPD) and also by pyridine adsorption (FTIR) method. Results are summarized in Table 1. It can be shown that the non-steamed GKF-3 catalyst which was prepared based on ZSM-5 has 0.233 mmol/g acidity, which is about 8 times higher than SB catalyst (based on Y-zeolite). Kaolin has much less acidity compared to GKF-3; but is almost double that of the SB catalyst. The ratio of Lewis acid and Bronsted acid was measured by FTIR (pyridine adsorption method). It can be seen, by referring, to Table 1, that kaolin contains no Bronsted acidity.

3.2. Conversion.

3.2.1. 1,3,5-Triisopropybenzene (1,3,5-TIPB). The cracking of 1,3,5-TIPB was investigated at variable temperature ranges (350, 400 and 450 ^{o}C) using two different catalysts of varying pore size (GKF-3 and SB) at 5,7,10 and 15 s reaction times. A comparative study was performed using kaolin catalyst at 400, 450 and 500 ^{o}C with reaction times (5,10 and 15 s). Results are given in Figures 3-4. It was observed that for both GKF-3 and SB catalysts and for all temperatures studied the conversion increases, as expected, with increase in reaction time (5-15 s). Figures 3a-3c show the temperature effect on 1,3,5-TIPB conversion. For instance, the conversion jumped from 13.17 % at 350 ^{o}C to 16.05 % at 400 ^{o}C, with an increase of 21.87 % using the GKF-3 catalyst. The corresponding change in conversion from 400 ^{o}C to 450 ^{o}C was 9.44 % with an increase of more than 58.8 %. The same phenomenon was observed with the SB catalyst even to a relatively higher degree. The conversion rose from 9.75 % at 350 ^{o}C to 19.03 % at 400 ^{o}C and to 27.59 % at 450 ^{o}C, corresponding to relative changes in conversion of 95.52 % and 45 % respectively. Kaolin on the other hand shows dependence of conversion on both temperature and residence time. However the effect of residence time on conversion was more profound compared to that of temperature. The effect of temperature on the 1,3,5-TIPB using kaolin is given in Figure 3c. It can be observed that increasing the

temperature for a set reaction time augmented the conversion up to 450 ^{o}C. A rise in temperature beyond 450 ^{o}C resulted in practically no change in conversion. A rise in temperature from 400 ^{o}C to 450 ^{o}C, using kaolin, raised the conversion of 1,3,5-TIPB from 15.14 % to 18.40 % for a 5 s residence time; corresponding to a conversion change from 28.63 % to 34.50 % for the same change in temperature change, and a 15 s residence time.

Figures 4 compares conversion of the 1,3,5-TIPB using different catalysts at 400 ^{o}C as a function of residence time. It is evident that kaolin with a bigger pore size (500-5000 Å) has always given higher conversions compared to the other two catalysts (GKF-3 and SB). This phenomenon can be attributed to the easy diffusion of the 1,3,5-TIPB, with 9.5 Å critical diameter, through kaolin and the diffusion limitations in case of the GKF-3 and the SB catalysts. Although the GKF-3 acidity is almost 8 times higher than that of the SB catalyst still they show comparable conversions at 400 ^{o}C (Figure 4) and 450 ^{o}C. This is an evidence that diffusional constrained molecules could still evolve in the 7.4 Å cage zeolite openings of the SB catalyst.[5] There is an evidence that the GKF-3 catalyst gives higher conversions compared to those obtained using the SB catalyst at 350 ^{o}C at all residence times tested. This trend was not noticed at higher temperatures studied (400 ^{o}C and 450 ^{o}C) and that conversions at these temperatures are comparable within experimental errors. This behavior can be explained based on the high diffusion activation energy of the 1,3,5-TIPB in the SB catalyst[5] bearing in mind that the 1,3,5-TIPB with 9.5 Å critical diameter can not diffuse through the GKF-3 catalyst, with relatively small pore size (5-6 Å).

3.2.2. 1,4-Diisopropybenzene (1,4-DIPB). Cracking of 1,4-DIPB was studied in a manner similar to that used in studying the 1,3,5-TIPB. The cracking of 1,4-DIPB was investigated at variable temperature ranges (350, 400 and 450 ^{o}C) using two different catalysts of varying pore size (GKF-3 and SB) at 5,7,10 and 15 s reaction times. Similar runs were made using a larger pore-size catalyst (kaolin) at 400, 450 and 500 ^{o}C) 5,10 and 15 s reaction times. It was observed, as expected, that in all cases the conversion increases with increase in reaction time and rise in temperature. However both temperature and reaction time dependence are different for the catalysts used. A summary of these results is given in Figures 5a through 6.

The GKF-3 catalyst showed moderate temperature dependence especially at low reaction times. For instance, at 5 s reaction time, the conversion increased from 11.30 % at 350 ^{o}C to 13.53 % at 400 ^{o}C and to 14.18 % at 450 ^{o}C; corresponding to 19.7 % increase from 350 ^{o}C to 400 ^{o}C and only 4.8 % increase from 400 ^{o}C to 450 ^{o}C. The corresponding figures obtained for the SB catalyst are 8.35 % conversion at 350 ^{o}C , 13.26 % at 400 ^{o}C and 13.30 % at 450 ^{o}C ; showing equal conversions at 400 and 450 ^{o}C respectively (Figure 5b). The conversion of 1,4-DIPB, using kaolin, shows lower temperature dependence. Figure 5c shows the effect of reaction time on 1,4-DIPB conversion, using kaolin, at 400 and 450 ^{o}C. Kaolin is not reactive at 350 ^{o}C.

Figure 6 compares the conversion of 1,4-DIPB using the catalysts under study at 450 ^{o}C. At 350 ^{o}C the GKF-3 gave higher conversions than the SB catalyst at all reaction times. This phenomenon is attributed to the comparatively high acidity of the GKF-3 compared to that of the SB catalyst despite the easy accessibility of the 1,4-DIPB molecules (6.8 Å) through the SB catalyst compared to that through the GKF-3. Figure 6 compares conversions for the three catalysts (GKF-3, SB and kaolin) at 450 ^{o}C. It can be noticed that the three catalysts give comparable conversions at 450 ^{o}C for 5 and 10 reaction times. The small difference, at 15 s reaction time and 450 ^{o}C, shown by the GKF-3 is within possible experimental errors. GKF-3 shows lower activity compared to the other two catalysts, at both 400 and 450 ^{o}C, especially for 15 s reaction time (Figure 6). It should be noted that SB and kaolin gave similar conversions of the 1,4-DIPB at 450 ^{o}C. This result is expected since both catalysts have low acidity with no diffusion constraints.

3.2.3. n-dodecane. n-dodecane is a straight chain hydrocarbon with 4.9 Å critical molecular diameter and hence n-dodecane can diffuse easily into the catalysts studied (GKF-3, SB and kaolin). Virtually no cracking was noticed using kaolin irrespective of reaction temperature or residence time. In fact, catalytic cracking of n-paraffins using kaolin, with low acidity, is a difficult task and inactivity of kaolin is expected. In an earlier study, Shendye and Rajadhyaksha emphasized the low crackability of n-paraffins as compared to other hydrocarbons.[29] It can also be seen by referring to Table 1 that kaolin, in contrast to other catalysts, has zero Bronsted acid sites. This explains the inactivity of kaolin in cracking n-dodecane, which needs Bronsted acid sites in order to

be cracked. For this reason only GKF-3 and SB catalysts were studied at varying temperatures and reaction times. Therefore the objective of this part of study is to eliminate the effect of diffusion constraints through the catalyst pores and study the effect of temperature and residence time on conversion for the GKF-3 and the SB catalysts. The study was performed at 350, 400, 450 ^{o}C temperatures and 5,7,10 and 15 s reaction times.

It was observed that for both catalysts and for all temperatures studied, the n-dodecane conversion increased with reaction time. Figure 7 is an example of this trend at 450 ^{o}C. Similar results were obtained at 350 and 400 ^{o}C. No noticeable moderation in this trend was noticed since no considerable coke formation was noticed for both catalysts at 450 ^{o}C for two reaction times, 5 and 10 s (Table 2). However in all runs the GKF-3 gave higher conversion rates of n-dodecane in comparison with the SB catalyst. The conversion using GKF-3 at 350 ^{o}C and 5 s residence time was 8.65 % while that of the SB catalyst, for the same conditions was only 0.57 % (about 15 folds). However this ratio is moderated at high temperatures and longer residence times. For instance at 450 ^{o}C and 15 s residence time this ratio drops to less than two folds, with 31.21 % and 15.98 % conversions respectively.

It might be worth mentioning that conversion of n-dodecane, using GKF-3, for the same residence time, has not changed after 400 ^{o}C reaction temperature On the other hand the SB catalyst, although gave lower conversions in comparison with the GKF-3 Catalyst (Figure 7), showed high conversion dependence on temperature even to an extended range of 500 ^{o}C. For instance the conversion jumped from 5.74 % at 400 ^{o}C to 8.69 % at 500 ^{o}C, for 5 s reaction time, and from 15.98 % to 20.04 % for 15 s reaction time, for the same temperature change (400 to 500 ^{o}C). It might be concluded that since no diffusion constraint is expected for n-dodecane, in both catalysts, the highly acidic GKF-3 will definitely give higher conversion compared to the SB catalyst.

3.2.4. Side Reactions. The appearance of xylenes and toluene in products of cracking 1,3,5-TIPB and 1,4-DIPB confirms that the propyl group associated with these two molecules can also be cracked into methyl groups (side chain cracking). Figures 8a and 8b show the effect of conversion of 1,3,5-TIPB and 1,4-DIPB, respectively, on methyl benzene yield (xylenes plus toluene). It is obvious that in both figures GKF-3 gave a higher yield of methyl benzene. Cracking the propyl group needs more activity

and hence GKF-3, being more acidic, is expected to crack the propyl group easier in comparison with SB and kaolin. The lack of Bronsted acid sites in case of kaolin is the main reason of the very low yield of the methyl benzene in cracking 1,3,5-TIPB and 1,4-DIPB using kaolin. On the other hand effect of conversion on methyl benzene yield is quite noticeable in case of GKF-3 specially in cracking 1,3,5-TIPB. The same trend can be noticed with 1,4-DIPB conversion. Furthermore extrapolation of both methyl benzene yields in both Figures 8a and 8b for all catalysts used does not pass through the zero origin. Consequently it can be concluded that side chain cracking of 1,3,5-TIPB and 1,4-DIPB (in the present condition) to produce methyl benzene is a secondary reaction.

3.3. Product Distribution and Selectivity.

3.3.1. 1,3,5-TIPB. The main products obtained by cracking the 1,3,5-TIPB are gases, mainly propylene, benzene, cumene, 1,3-DIPB and some isomers of TIPB. The product distribution of cracking 1,3,5-TIPB confirms the domination of the three step series reactions suggested by Al-Khataf and de Lasa.[4]: (a) dealkyulation of 1,3,5-TIPB to form 1,3-DIPB and propylene, (b) dealkylation of 1,3-DIPB to give cumene and propylene, (c) dealkylation of cumene to form benzene. Beside these dominant steps there are side reactions such as disproportionation, isomerization and condensation that may affect gas phase product distribution and coke formation.[11,12] The extent of these steps depends on reaction conditions and catalyst geometry and composition.[12]

The effect of catalyst type and operating conditions on product distribution and selectivity, for cracking 1,3,5-TIPB, will be discussed based on the experimental findings (Figure 9).

The effect of 1,3,5-TIPB conversion, at 450 ^{o}C, on 1,3- DIPB selectivity (first dealkylation step) is given in Figure 9a. For all temperatures studied the selectivity of 1,3-DIPB shows dependence on 1,3,5-TIPB conversion. Kaolin with the highest conversion of 1,3,5-TIPB (Figure 4) has shown highest selectivity as well. This result is quite expected since no diffusion constraints are associated with kaolin compared with the GKF-3 and the SB catalysts. However it can be noticed that the GKF-3 which gave comparable conversions with SB (Figure 4), has shown higher selectivity of 1,3-DIPB compared with the SB catalyst at all temperatures. This can be explained by the fact that the 1,3-DIPB with 8.4 Å critical diameter[4] can diffuse easily through the SB catalyst to

produce cumene, while in case of GKF-3 the first dealkylation step takes place on the external surface area and the produced 1,3-DIPB is still too large to diffuse inside the ZSM-5 pores structure. Figure 9b is a plot of temperature effect on 1,3-DIPB selectivity for 5 s reaction time. The plot shows that the selectivity of 1,3-DIPB drops sharply with temperature in case of kaolin due to the high rate of cracking 1,3-DIPB to form cumene. For instance the selectivity dropped from 27.75 % at 400 ^{o}C to 18.15 % at 450 ^{o}C for 5 s reaction time. The selectivity for the same molecule (1,3-DIPB) dropped from 32.34 % at 400 ^{o}C to 27.07 % at 450 ^{o}C, then to only 14.06 % at 500 ^{o}C for a reaction time of 15 s.

GKF-3 and SB catalysts have shown much lower selectivity of 1,3-DIPB compared to kaolin. For the same temperature range, 350 ^{o}C, 400 ^{o}C and 450 ^{o}C the selectivity of the 1,3-DIPB using GKF-3 changed from 8.44 % to 11 % and then dropped to 6.57 % showing maximum selectivity at 400 ^{o}C. The same phenomenon was noticed in using the SB catalyst with corresponding selectivity of 1.05 %, 4.56 % and 1.34 % at 350, 400 and 450 ^{o}C respectively, again showing a maximum at 400 ^{o}C. In fact the selectivity of 1,3-DIPB is governed by the rate of cracking the 1,3,5-TIPB to produce 1,3-DIPB and the rate of cracking the 1,3-DIPB to produce cumene and propylene.

Effect of 1,3,5-TIPB conversion on cumene selectivity (second dealkylation step), at 400 ^{o}C, is given in Figure 10a. It should be noted that the GKF-3 catalyst has always shown the lowest selectivity of cumene and almost no conversion dependence (Figure 10a). Similar trends were noticed for other temperatures studied. On the other hand the selectivity of cumene using SB catalyst is higher than that using the GKF-3 and shows high dependence on 1,3,5-TIPB conversion. Kaolin has shown insignificant conversion dependence both at 400 and 450 ^{o}C. Figure 10b shows the dependence of cumene selectivity on temperature using different catalysts for a 5 s reaction time. The plot shows a very moderate dependence on temperature in case of the GKF-3 catalyst and high dependence in case of kaolin. The selectivity of cumene increases with increase in temperature in case of kaolin. It should be recalled that the behavior was completely different in case of 1,3-DIPB selectivity for the same catalyst. The SB has shown an increase in cumene selectivity from 3 % at 350 ^{o}C to 9.85 % at 400 ^{o}C and a drop to 8.52 % at 450 ^{o}C. A similar behavior was noticed when discussing the 1,3-DIPB selectivity (Figure 9b). It has to be emphasized that both 1,3-DIPB and cumene are intermediate

products of 1,3,5-TIPB cracking. Thus the trend of showing maxima in their selectivity would be expected.

Benzene is the third step in the dealkylation series in cracking the 1,3,5-TIPB. In general and for all catalysts selectivity has shown temperature dependence (Figure 11c). Temperature augments benzene selectivity; but to different degrees for the three catalysts studied. Kaolin showed the lowest selectivity compared with the GKF-3 and the SB catalysts. The GKF-3 gave highest selectivity moderating at higher temperatures, giving comparable conversion with SB at 450 ^{o}C for a 5 s reaction time. The difference in benzene selectively for the same catalysts is quite noticeable at 350 ^{o}C. A big difference in selectivity of benzene was obtained at 350 ^{o}C for the same catalysts; 11.71 % and 5.43 % using GKF-3 and SB respectively (Figure 11b). On the other hand Figure 11a shows minor dependence of selectivity on 1,3,5-TIPB conversion at 450 ^{o}C. The same trend was noticed at 400 ^{o}C. Kaolin has always given lower selectivity of benzene and higher 1,3,5-TIPB conversions compared to the other two catalysts. It should be noted that both GKF-3 and SB catalysts gave comparable values of benzene selectivity at 450 ^{o}C. The high benzene selectivity for GKF-3 might be attributed to the adsorption of benzene ring on the external acid sites. However in case of kaolin, adsorption might take place via the propyl group leading to formation of 1,3-DIPB and cumene.

3.3.2. 1,4-DIPB. The main products of 1,4-DIPB reaction are gases, cumene, benzene and DIPB isomers. Other products seen in small amounts were xylenes and toluene. Tetra-isopropyl-benzene was detected in case of cracking 1,4-DIPB using kaolin. The product distribution suggests that the main reaction is the two-step dealkylation of 1,4-DIPB to form cumene and propene followed by cracking the formed cumene to give benzene and propene. Beside these dominant steps there are side reactions such as disproportionation, isomerization and alkylation to form tetra-isoppropyl-benzene.[4]

Cumene is the first step in the dealkylation series. Figure 12a shows the effect of conversion of 1,4-DIPB on cumene selectivity at 450 ^{o}C. It can be noted that the cumene selectivity depends, on both, type of catalyst and temperature (Figure 12a and 12b). However in all cases kaolin has shown higher selectivity, followed by the SB and the GKF-3 has always shown lowest selectivity of cumene. Both GKF-3 and SB catalysts have shown maximum selectivity at 400 ^{o}C after which a noticeable drop can be seen.

The same conclusion can be drawn in case of kaolin since kaolin is not reactive at 350 ^{o}C. This trend is clear in Figure 12b where the comparison is performed for a 5 s reaction tine. Extrapolation of results for kaolin (not shown in Figure) show that the selectivity of cumene drops from 50.5 % to 47.19 % and then to 39.79 % for temperatures of 400, 450 and 500 ^{o}C, and for 15 s reaction time, respectively.

The above trends are completely reversed in case of benzene selectivity in the sense that in all cases kaolin gave the lowest selectivity, followed by the SB catalyst and the GKF-3 gave highest benzene selectivity all through (Figure 13). This trend is expected since production of benzene is on the expense of cumene conversion to benzene (second dealkylation step). It can also be noted that the selectivity of benzene shows minor dependence on the 1,4-DIPB conversion (Figure 13a) at 400 ^{o}C. Similar results were obtained at 450 ^{o}C. In all cases and for the three catalysts the selectivity of benzene is augmented with rise in temperature (Figure 13b). High selectivity of benzene using GKF-3 and low selectivity using kaolin can be explained in a manner similar to that used in the previous section (1,3,5-TIPB).

3.3.3. Coke Yield

Regarding coke formation on different catalysts, the three catalysts were tested for coke formation at the same conditions (T = 450 ^{o}C, and two reaction times 5 and 10 s). Table 2 reports coke yield for each molecule and catalyst. It can be noticed that for both GKF-3 and SB catalysts 1,3,5-TIPB produces more coke than the other two molecules. For example, using SB catalyst, the amount of coke produced at 10 sec reaction time was 0.34, 0.26 and 0.15 wt % for 1,3,5-TIPB, 1,4-DIPB, and n-dodecane respectively. It is well established that olefins and polynuclear aromatics have high tendency to form coke.[7] This can explain why 1,3,5-TIPB produces more coke than the other two model compounds used in the present study. Furthermore, Corma and Wojciechowski[7] in the same study attributed coke formation, in cumene catalytic cracking, mainly to propene. Thus the high propene yield, when cracking 1,3,5-TIPB, can explain the high coke yield associated with cracking this molecule.

Furthermore, coke formation in case of 1,3,5-TIPB was found to be more sensitive to reaction time than the other molecules. Figure 14 depicts that kaolin produces much less coke than both GKF-3 and SB catalysts. This result is quite

interesting because kaolin has higher acidity than SB catalyst and much less acidity than the GKF-3 catalyst. Thus the low coke yield in case of kaolin has to do with acid type and strength. Furthermore, due to the incomplete dealkylation process in case of kaolin, propene yield is less than the other two zeolite catalysts. This confirms that coke formation increases with propene yield. The gas yield, from cracking 1,3,5-TIPB at 450 ^{o}C, is lower in case of kaolin in comparison with SB and GKF-3; and hence kaolin would be expected to give lower coking as well.

4. Conclusions

Cracking of 1,3,5-TIPB, 1,4-DIPB and n-dodecane using ZSM-5 (GKF-3), Y-Zeolie (SB) and kaolin catalysts, of different pore size, was successfully performed in a novel CREC Riser Simulator under different reaction times and temperatures. Kaolin with the biggest pore size has always given higher conversion of 1,3,5-TIPB compared with SB catalyst and GKF-3 catalysts. The conversion of 1,3,5-TIPB, for all catalysts as expected, is augmented by temperature rise and increase in residence time. Due to the absence of Bronsted acidity, kaolin is not reactive in case of n-dodecane. The relatively high acidic GKF-3 catalyst gave higher n-dodecane conversion than SB.

Regarding the selectivity of 1,3-DIPB, obtained by cracking 1,3,5-TIPB, kaolin has also shown higher selectivity of 1,3-DIPB compared with GKF-3. SB has shown the lowest selectivity of 1,3-DIPB at all 1,3,5-TIPB conversion ranges. Both GKF-3 and SB have shown maximum selectivity of 1,3-DIPB at 400 ^{o}C. Kaolin has shown a sharp drop in 1,3-DIPB selectivity, at 5 s reaction time, between 400 ^{o}C and 450 ^{o}C reaction temperatures. GKF-3 has given lowest selectivity of cumene from cracking 1,3,5-TIPB and almost constant with temperature at 5 s reaction time. Unlike the 1,3-DIPB selectivity, kaolin has shown an increase in cumene selectivity, at 5 s reaction time, between 400 ^{o}C and 450 ^{o}C reaction temperatures.

As expected and since kaolin gave higher selectivity for both 1,3-DIPB and cumene, the selectivity of benzene was lowest using kaolin and higher for SB and GKF-3 catalysts which gave comparable selectivity of benzene at 450 ^{o}C from cracking 1,3,5-TIPB. Cumene selectivity by cracking 1,4-DIPB is highest using kaolin and lowest in

case of GKF-3 with the smallest pore size. Selectivity of cumene showed little dependence on 1,4-DIPB conversion. GKF-3, on the other hand, gave higher benzene selectivity from cracking 1,4-DIPB and kaolin gave lowest selectivity. In all case selectivity of benzene is increased with increase in temperature for 5 s reaction time.

Acknowledgement

The authors gratefully acknowledge King Fahd University of Petroleum & Minerals for the financial support provided for this work under the project ARI-029. Also we would like to thank Mr. Mariano Gica for his invaluable assistance in the experimental part of this work. Special thank are due to Dr. Shakeel Ahmed and Mr Khurshid Alam for their invaluable assistance and suggestions.

References

(1) Rossini, Stefano, Catalysis Today, 77, **2003**, 467-484.

(2) Karger, J., & Ruthven, D.M. John Wiley & Sons, Inc. **1992**.

(3) Al-Khattaf, S. Ph.D Dissertation, University of Western Ontario, London, Ontario, Canada, **2001**.

(4) Al-Khattaf, S. & de Lasa, H. Applied Catalysis A General, **2002,** 226, 139-153

(5) Al-Khattaf, S.; Atias, J.A; Jarosch, K.; de Lasa, H. Chemical Engineering Science, **2002**, 57, 4909.

(6) Xiao, J.; Wei, J. Chem Eng Sci. **1992**, 47, 5, 1123-1141.

(7) Corma, A.; Wojciechowski, B.W. Cat. Rev. Sci. Eng. **1982**, 24, 1, 1-65.

(8) Roos, K.; Liepoid, A.; Koch, H., and Reschetilowski, W. Chem. Eng . Technol. **1997**, 20, 326-332.

(9) Rajagopalan, K.; Young, G.W. Prepr.-Am. Soc., Div. Pet. Chem. **1987**, 32, 3, 627.

(10) Biswas, J.; Maxwell, I. E. Appl. Catal. **1990**, 58, 1.

(11) Madon,R. J. J. Catal. **1991**, 129, 275.

(12) Elia, M. F. ; Iglesias, E.; Martinez, A.; Pascual, M.A. Appl. Catal. **1991**, 73, 195.

(13) Miller,S. J.; Hsieh, C.R. Prepr.-Am. Chem. Soc. Div. Pet. Chem. **1990**, 685.

(14) Nalbandian, L.; Vasalos, I.A.; Kasapaki, A.; Vassilakis, K. Prepr.Am. Chem. Soc., Div. Pet. Chem. **1993**, 584.

(15) Guerzoni, F.N.; Abbot, J. Appl. Catal. A **1994**, 120, 55.

(16) Nalbandian, I.; Lemonidou, A.A.; Vasalos, I.A. Appl. Catal. A. **1993**, 105, 107.

(17) Donnelly, S.P.; Mizrahi, S.; Sparrell, P.T.; Huss, A. Jr; Schipper,P.H.; Herbst, J.A. Prepr.Am. Chem. Soc., Div. Pet. Chem. **1987**, 32 (3), 621.

(18) Dwyer, J.; Rawlence, D.J. Catal . Today, **1997**, 18, 487.

(19) Buchanan J.S. Catalysis Today, **2000**, 55, 207-212.

(20) Biswas, J.; Maxwell, I.E. Applied Catalysis A, **1990**, 63, pp 197-258.

(21) Aitani, A.; Yoshikawa, T.; Ino, T. Catalysis Today, **2000**, 60, 111-117.

(22) Herrman, C.; Haas, J.; Fetting, F. Applied Catalysis, **1987**, 35, 299-310.

(23) Corma, A.; Melo, F.; Sauvanaud, L.; Ortega, F. Applied Catalysis A: General 265, **2004**, 195-206.

(24) de Lasa, H.I. U.S. Pat. 5 102 628, **1992** .

(25) Iliyas, A.; Al-Khattaf, S. Ind. Eng. Chem. Res., 43, **2004**, 1349.

(26) Iliyas, A.; Al-Khattaf, S. Appl. Catal. A: Gen 269, **2004**, 225-236.

(27) Kraemer, D.W. Ph.D. Dissertation, University of Western Ont., London, Canada, **1991**.

(28) Haag, W.O., Lago, R.M., and Weisz, P.B. Discuss. Faraday Soc. **1981**, 72, 317.

(29) Shendye, R.V.; Rajadhyaksha, R.A.Chemical engineering Science, Vol. 47, **1992**, No. 3, pp.653-659.

List of Tables

Table 1. Characterization of used Catalysts

Catalyst	Acidity (mmol/g)	Lewis sites %	Bron sites %	Surface Area (m^2/g)	Catalyst Type	Na_2O wt %
GKF-3	0.233	44	56	70	ZSM-5	Negligible
SB	0.03	35	65	150	Y-Zeolite	Negligible
Kaolin	0.07	100	0	14	Amorphous	Negligible

Table 2. Coke Analysis: Cracking of 1,3,5-TIPB, 1,4-DIPB & n-dodecane using GKF-3, SB & Kaolin Catalysts

Catalyst	Molecule	Residence Time (s)	Total Carbon (wt %)
GKF-3	n-dodecane	5	0.15
GKF-3	n-dodecane	10	0.15
GKF-3	1,4-DIPB	5	0.19
GKF-3	1,4-DIPB	10	0.19
GKF-3	1,3,5-TIPB	5	0.22
GKF-3	1,3,5-TIPB	10	0.32
FCC.B	n-dodecane	5	0.10
FCC.B	n-dodecane	10	0.15
FCC.B	1,4-DIPB	5	0.21
FCC.B	1,4-DIPB	10	0.21
FCC.B	1,3,5-TIPB	5	0.26
FCC.B	1,3,5-TIPB	10	0.34
Kaolin	1,4-DIPB	5	0.06
Kaolin	1,4-DIPB	10	0.09
Kaolin	1,3,5-TIPB	5	0.08
Kaolin	1,3,5-TIPB	10	0.16

List of Figures

Figure 9a. Effect of 1,3,5-TIPB conversion on 1,3-DIPB selectivity at 450 ^{o}C

◆ GKF-3 catalyst □ SB catalyst ▵ Kaolin catalyst

Figure 9b. 1,3,5-TIP cracking: Effect of temperature on 1,3-DIPB selectivity, reaction time = 5 s ◆ GKF-3 □ SB ▵ Kaolin

Figure 10a. Effect of 1,3,5-TIPB conversion on cumene selectivity at 400 ^{o}C

◆ GKF-3 □ SB ▵ Kaolin

Figure 10b. 1,3,5-TIPB cracking: Effect of temperature on cumene selectivity, reaction time = 5 s ◆ GKF-3 □ SB ▵ Kaolin

Figure 11a. Effect of 1,3,5-TIPB conversion on benzene selectivity at 450 ^{o}C

◆ GKF-3 □ SB ▵ Kaolin

Figure 11b. 1,3,5-TIPB cracking: Effect of temperature on benzene selectivity, reaction time = 5 s ◆ GKF-3 □ SB ▵ Kaolin

Figure 12a. Effect of 1,4-DIPB conversion on cumene selectivity at 450 ^{o}C

◆ GKF-3 □ SB ▵ Kaolin

Figure 12b. 1,4-DIPB cracking: Effect of temperature on cumene selectivity, reaction time = 5 s ◆ GKF-3 □ SB ▵ Kaolin

Figure 13a. Effect of 1,4-DIPB conversion on benzene selectivity at 400 ^{o}C

◆ GKF-3 □ SB ▵ Kaolin

Figure 13b. 1,4-DIPB cracking: Effect of temperature on benzene selectivity, reaction time = 5 s ◆ GKF-3 □ SB ▵ Kaolin

Figure 14 Effect of 1,3,5-TIPB conversion on coke yield at 450 ^{o}C

◇ GKF-3 ■ SB ▵ Kaolin

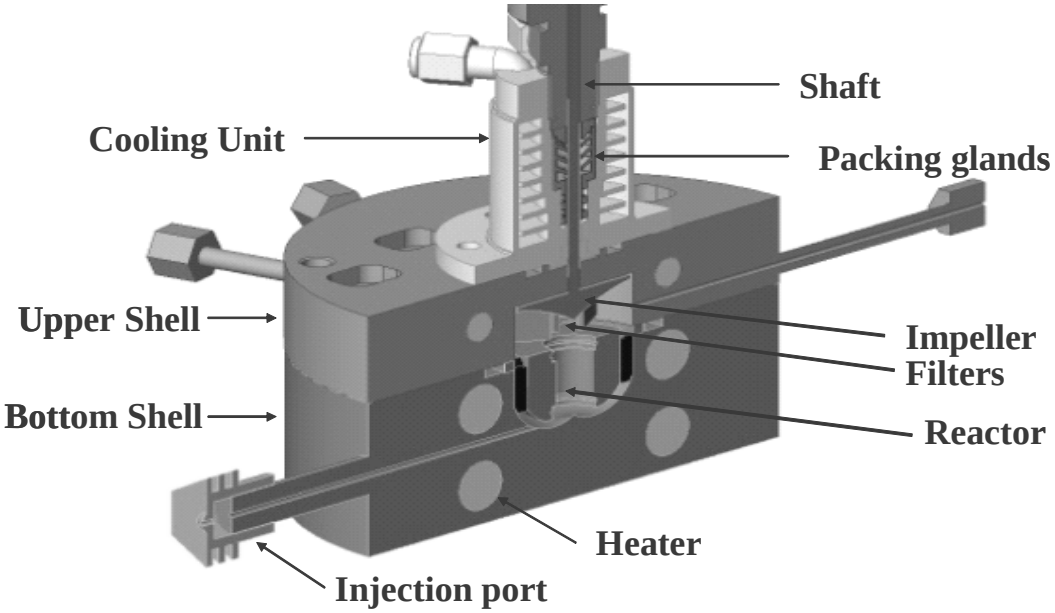

Figure 1. Schematic diagram of the Riser Simulator

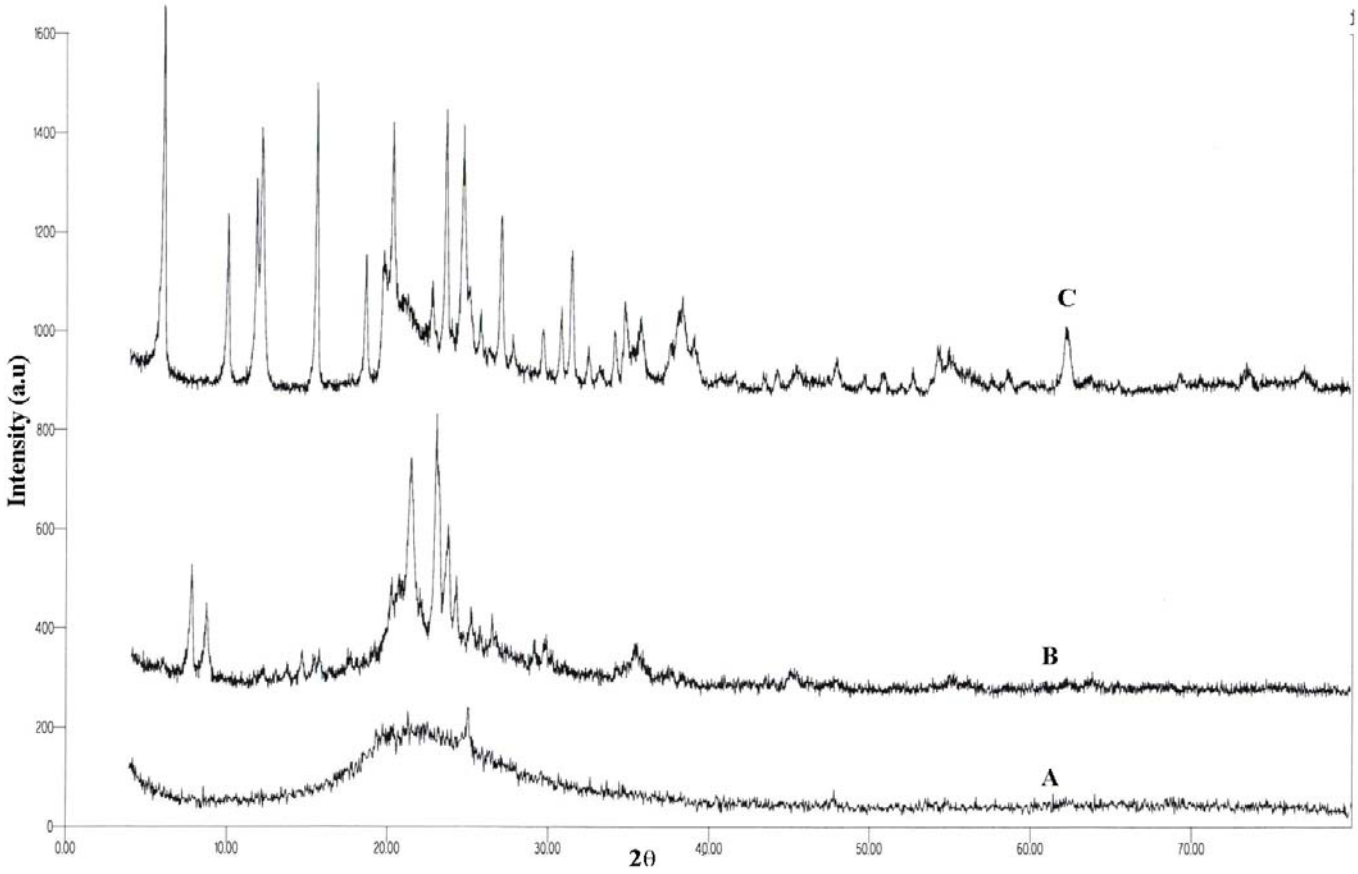

Figure 2. X-ray Diffraction for the Catalysts used in the Present Study

A: Kaolin Catalyst B: GKF-3 Catalyst C: SB Catalyst

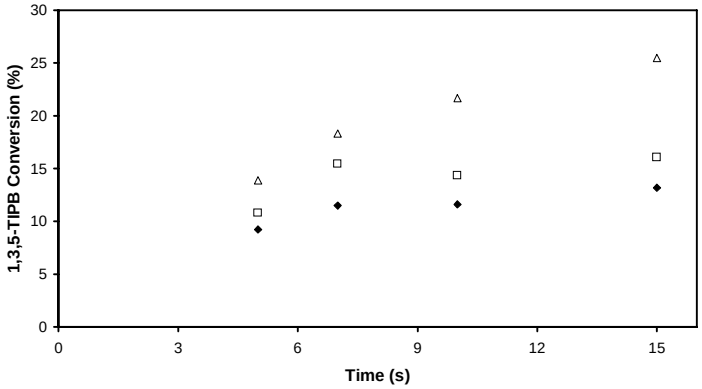

Figure 3a. 1,3,5-TIPB conversion vs reaction time using GKF-3 catalyst
◆ 350 °C □ 400 °C △ 450 °C

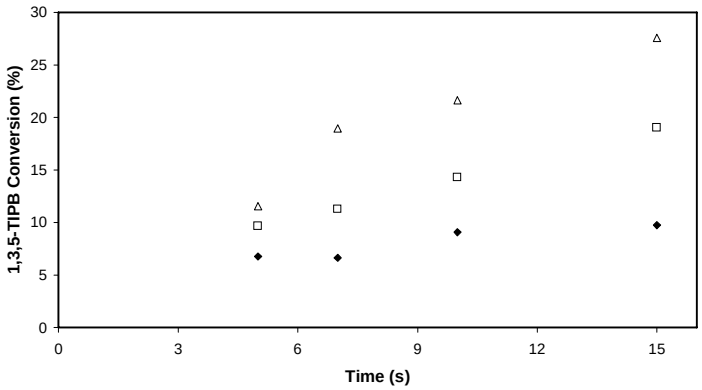

Figure 3b. 1,3,5-TIPB conversion vs reaction time using SB catalyst
◆ 350 °C □ 400 °C △ 450 °C

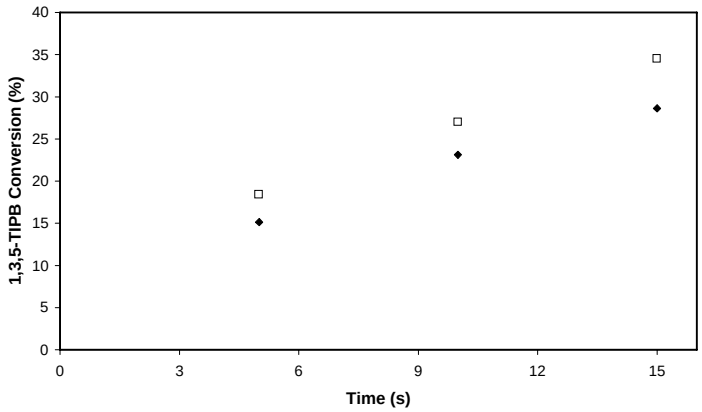

Figure 3c. 1,3,5-TIPB conversion vs reaction time using kaolin catalyst

◆ 400 ^{o}C □ 450 ^{o}C

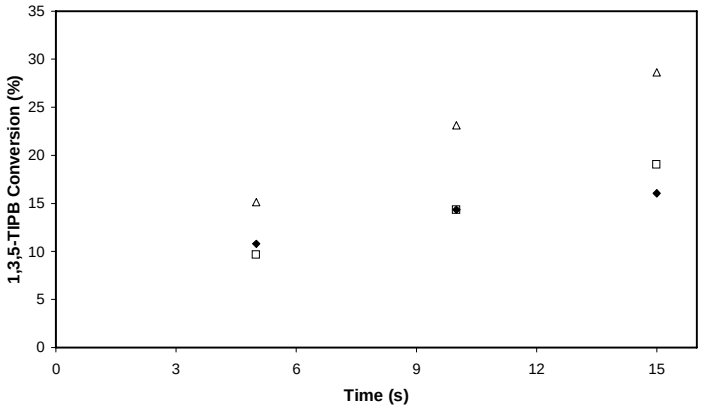

Figure 4. Conversion of 1,3,5-TIPB at 400 ^{o}C using different catalysts
◆ GKF-3 □ SB △ Kaolin

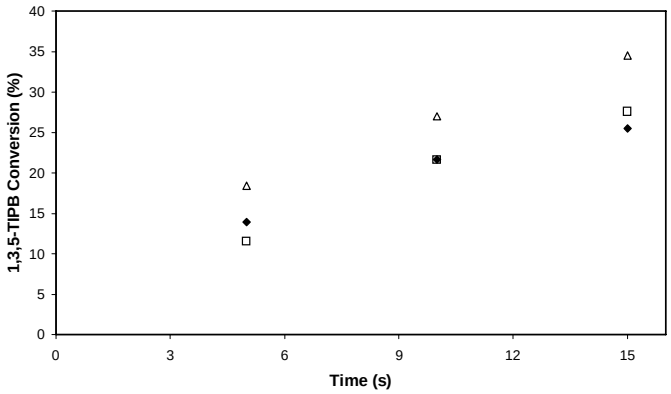

Figure 5a. 1,4-DIPB conversion vs reaction time using GKF-3 catalyst
◆ 350 ^{o}C □ 400 ^{o}C △ 450 ^{o}C

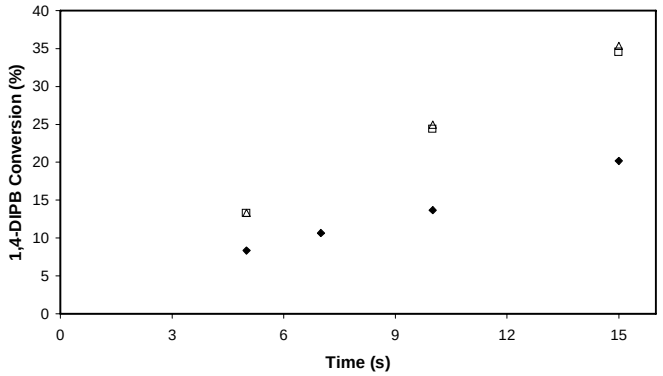

Figure 5b. 1,4-DIPB conversion vs reaction time using SB catalyst
◆ 350 ^{o}C □ 400 ^{o}C △ 450 ^{o}C

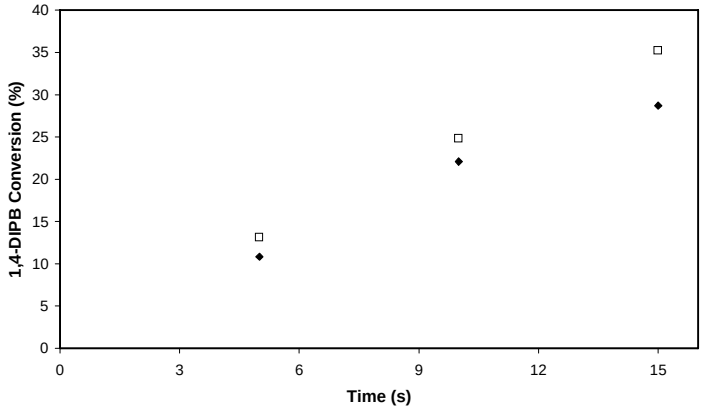

Figure 5c. 1,4-DIPB conversion vs reaction time using kaolin catalyst

◆ 400 ^{o}C □ 450 ^{o}C

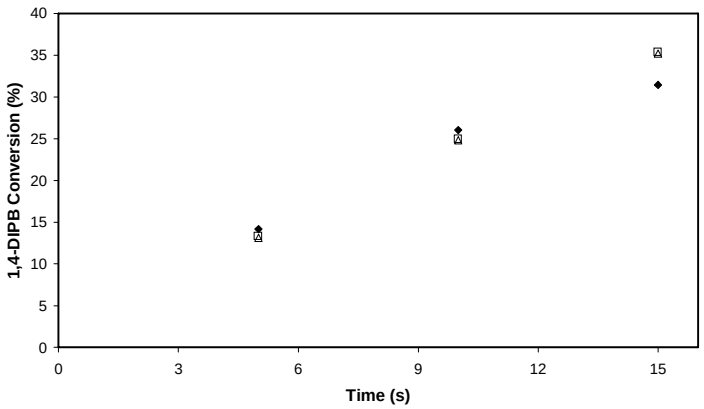

Figure 6. Conversion of 1,4-DIPB at 450 ^{o}C using different catalysts

◆ GKF-3 □ SB ▵ Kaolin

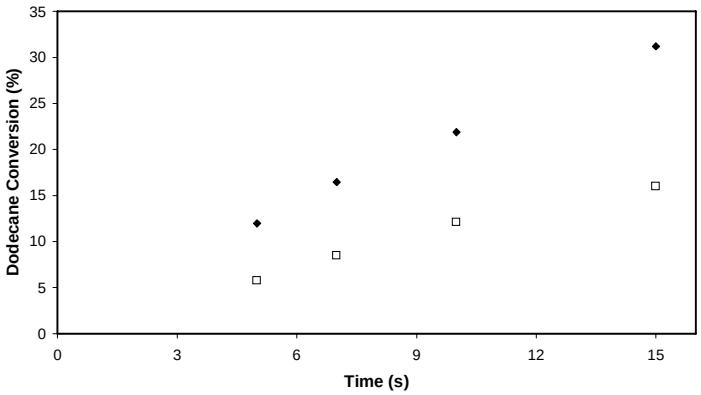

Figure 7. Conversion of n-dodecane at 450 ^{o}C using different catalysts
◆ GKF-3 □ SB

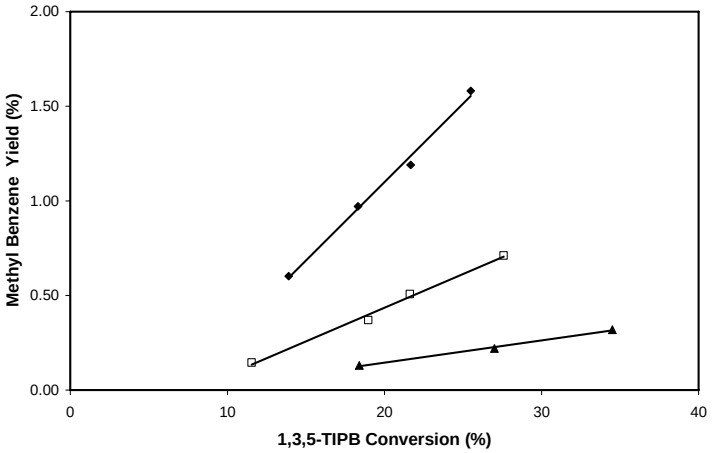

Figure 8a. Effect of 1,3,5-TIPB conversion on methyl benzene yield at 450 ^{o}C.
◆ GKF-3 catalyst □ SB catalyst ▲ Kaolin catalyst

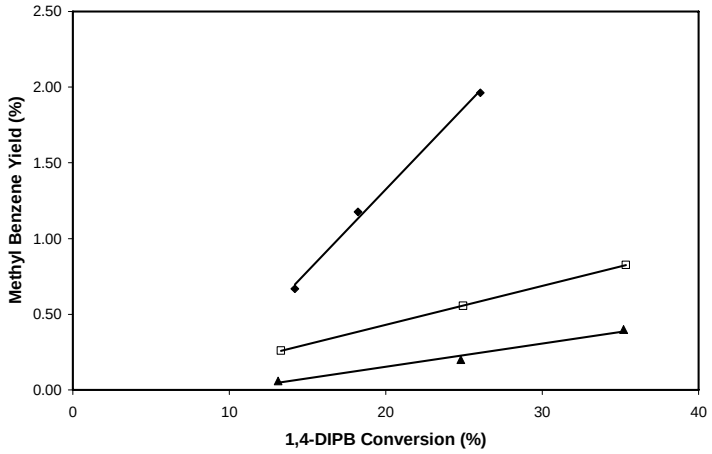

Figure 8b. Effect of 1,4-DIPB conversion on methyl benzene yield at 450 ^{o}C.
◆ GKF-3 catalyst □ SB catalyst ▲ Kaolin catalyst

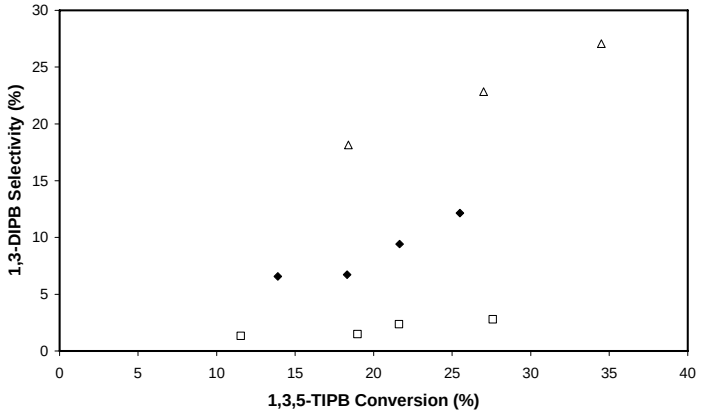

Figure 9a. Effect of 1,3,5-TIPB conversion on 1,3-DIPB selectivity at 450 ^{o}C
◆ GKF-3 catalyst □ SB catalyst △ Kaolin catalyst

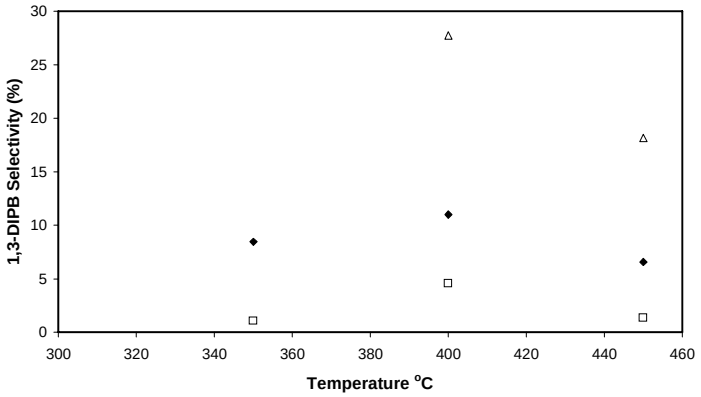

Figure 9b. 1,3,5-TIP cracking: Effect of temperature on 1,3-DIPB selectivity, reaction time = 5 s ◆ GKF-3 □ SB △ Kaolin

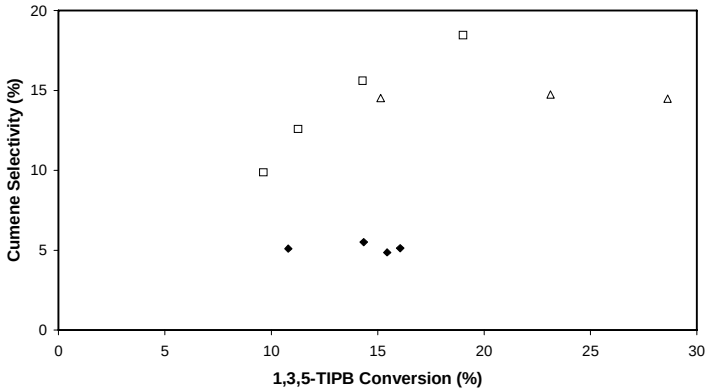

Figure 10a. Effect of 1,3,5-TIPB conversion on cumene selectivity at 400 ^{o}C
◆ GKF-3 □ SB △ Kaolin

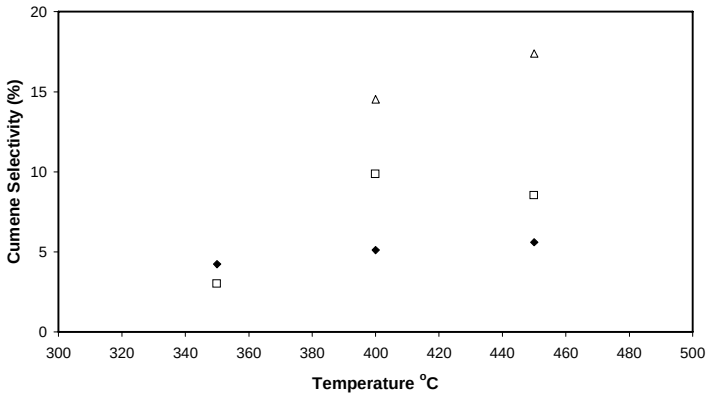

Figure 10b. 1,3,5-TIPB cracking: Effect of temperature on cumene selectivity, reaction time = 5 s ◆ GKF-3 □ SB △ Kaolin

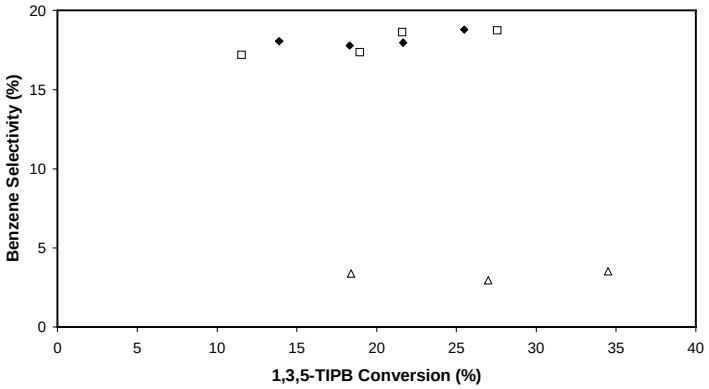

Figure 11a. Effect of 1,3,5-TIPB conversion on benzene selectivity at 450 ^{o}C
◆ GKF-3 □ SB △ Kaolin

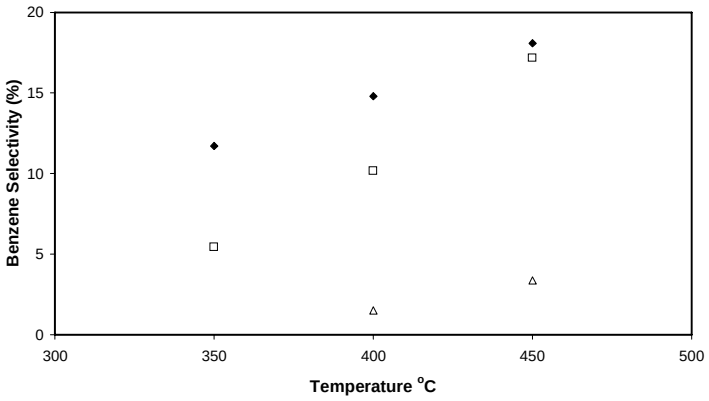

Figure 11b. 1,3,5-TIPB cracking: Effect of temperature on benzene selectivity, reaction time = 5 s ◆ GKF-3 □ SB △ Kaolin

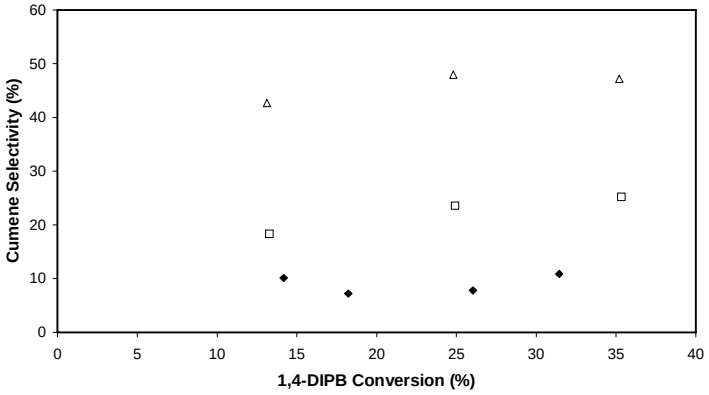

Figure 12a. Effect of 1,4-DIPB conversion on cumene selectivity at 450 ^{o}C

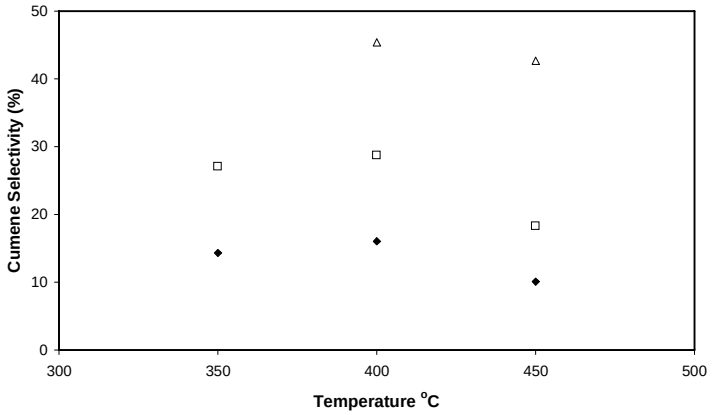

◆ GKF-3 □ SB ▵ Kaolin

Figure 12b. 1,4-DIPB cracking: Effect of temperature on cumene selectivity, reaction time = 5 s ◆ GKF-3 □ SB ▵ Kaolin

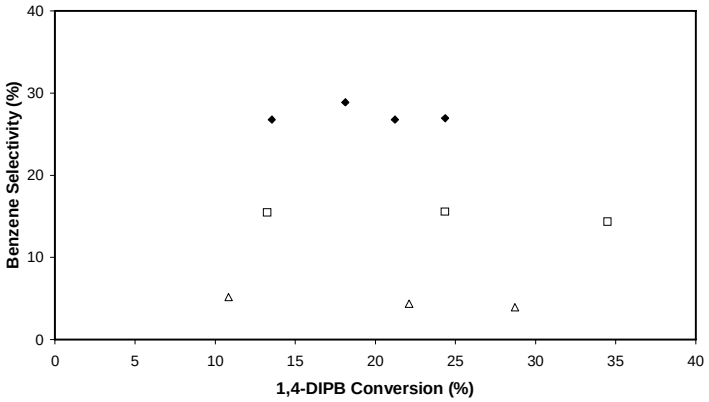

Figure 13a. Effect of 1,4-DIPB conversion on benzene selectivity at 400 ^{o}C
◆ GKF-3 □ SB △ Kaolin

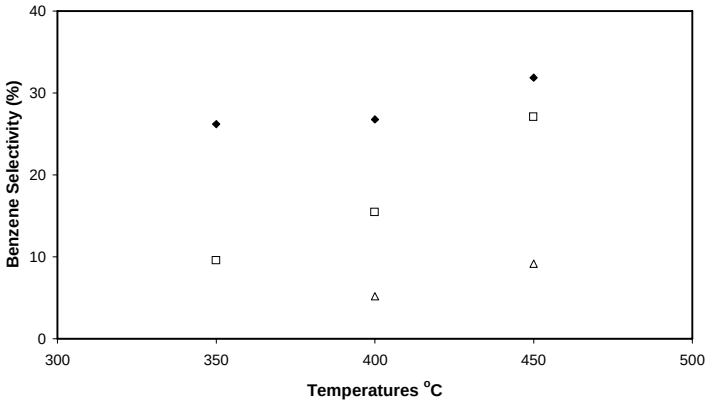

Figure13b. 1,4-DIPB cracking: Effect of temperature on benzene selectivity, reaction time = 5 s ◆ GKF-3 □ SB △ Kaolin

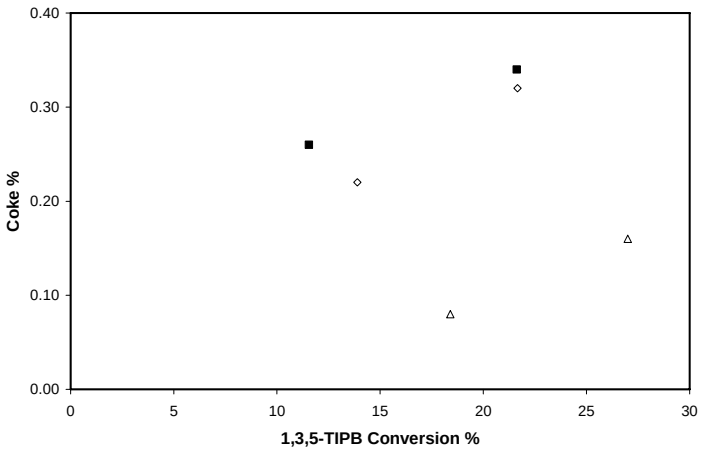

Figure 14. Effect of 1,3,5-TIPB conversion on coke yield at 450 ^{o}C

◇ GKF-3 ■ SB △ Kaolin